HHS Public Access

Author manuscript

*Cell Rep*. Author manuscript; available in PMC 2022 June 08.

Published in final edited form as:

*Cell Rep*. 2022 May 17; 39(7): 110820. doi:10.1016/j.celrep.2022.110820.

# FMRP regulates $GABA_A$ receptor channel activity to control signal integration in hippocampal granule cells

**Pan-Yue Deng**[1], **Ajeet Kumar**[2], **Valeria Cavalli**[2,3,4], **Vitaly A. Klyachko**[1,3,5,*]

[1]Department of Cell Biology and Physiology, Washington University School of Medicine, St Louis, MO 63110, USA

[2]Department of Neuroscience, Washington University School of Medicine, St Louis, MO 63110, USA

[3]Hope Center for Neurological Disorders, Washington University School of Medicine, St Louis, MO 63110, USA

[4]Center of Regenerative Medicine, Washington University School of Medicine, St Louis, MO 63110, USA

[5]Lead contact

## SUMMARY

Fragile X syndrome, the most common inherited form of intellectual disability, is caused by loss of fragile X mental retardation protein (FMRP). GABAergic system dysfunction is one of the hallmarks of FXS, yet the underlying mechanisms remain poorly understood. Here, we report that FMRP interacts with $GABA_A$ receptor ($GABA_AR$) and modulates its single-channel activity. Specifically, FMRP regulates spontaneous $GABA_AR$ opening through modulating its single-channel conductance and open probability in dentate granule cells. FMRP loss reduces spontaneous $GABA_AR$ activity underlying tonic inhibition, while N-terminal FMRP fragment (aa 1–297) is sufficient to rapidly normalize tonic inhibition in *Fmr1* knockout (KO) granule cells. FMRP-$GABA_AR$ interaction is supported by co-immunoprecipitation of FMRP with at least one $GABA_AR$ subunit, the α5. Functionally, FMRP-$GABA_AR$ interaction ensures accuracy of coincidence detection of granule cells, which is markedly reduced in *Fmr1* KOs. Our study reveals a mechanism underlying FMRP regulation of the GABAergic system and information processing in the hippocampus.

## In brief

*Correspondence: klyachko@wustl.edu.

AUTHOR CONTRIBUTIONS

P.-Y.D. and V.A.K. conceived and designed the experiments. P.-Y.D. performed all electrophysiological studies and analyzed the data. A.K. and V.C. designed coIP experiments, and A.K. performed these experiments. All authors wrote the manuscript and approved the final version.

DECLARATION OF INTERESTS

The authors declare no competing interests.

SUPPLEMENTAL INFORMATION

Supplemental information can be found online at https://doi.org/10.1016/j.celrep.2022.110820.

Deng et al. report that FMRP interacts with GABAA receptors and regulates their single-channel activity. Functionally, this interaction controls tonic inhibition to ensure accurate signal integration in hippocampal granule cells. These findings reveal a mechanism underlying FMRP regulation of the GABAergic system and information processing in the hippocampus.

## Graphical Abstract

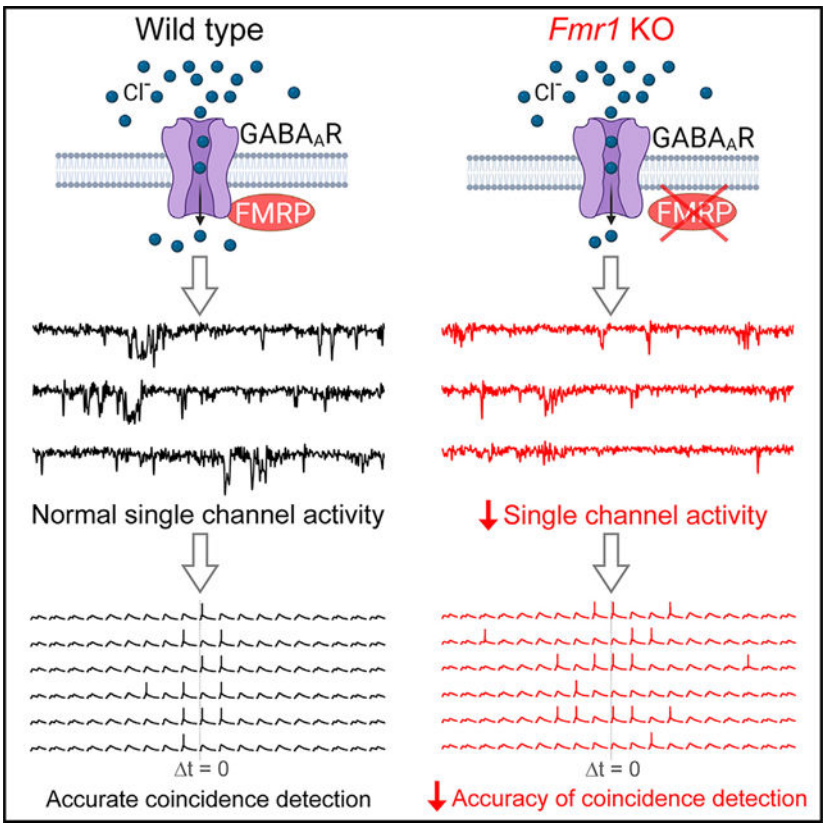


## INTRODUCTION

Fragile X syndrome (FXS) is the leading monogenic cause of intellectual disability, which stems from mutations in the *Fmr1* gene resulting in a loss of fragile X mental retardation protein (FMRP) (Salcedo-Arellano et al., 2020). Accumulating evidence implicates dysfunction of the GABAergic system as one of the major contributing factors to neural circuit deficits and clinical abnormalities in FXS (Van der Aa and Kooy, 2020). Over half of $GABA_A$ receptor ($GABA_AR$) subunits are reported to be affected at the protein level in FXS models and patients (Van der Aa and Kooy, 2020). Targeting the GABAergic system also showed promising therapeutic potential in animal studies (Lozano et al., 2014). Unfortunately, clinical trials failed to reach significant improvements in FXS individuals, suggesting that better understanding of the mechanisms underlying GABAergic system dysfunction are needed for successful development of GABAergic-system-based interventions.

The GABAergic system modulates activity of neural networks through two distinct modes, phasic inhibition and tonic inhibition, which are mediated by the synaptic and extrasynaptic GABAARs, respectively (Tang et al., 2021). Phasic inhibition plays a critical role in rapid time-locked feed-forward and feedback inhibition, while tonic inhibition acts persistently to shape signal integration via its hyperpolarizing and shunting effects. The phasic $GABA_AR$s have a high density at synapses, but the extrasynaptic tonic $GABA_AR$s are much more abundant overall because synapses constitute only a small part of the cell surface (<1%) (Kasugai et al., 2010). Moreover, unlike phasic inhibition, tonic conductance is continuously active, and ~95% of total $GABA_AR$ charge transfer is attributed to tonic conductance (O'Neill and Sylantyev, 2018). A number of studies have identified abnormalities of tonic inhibition in various brain regions of FXS mouse models (Curia et al., 2009; D'Hulst et al., 2006; Martin et al., 2014; Modgil et al., 2019; Olmos-Serrano et al., 2010, 2011; Whissell et al., 2015; Zhang et al., 2017), yet the underlying mechanisms, as well as physiological consequences, of these defects remain poorly understood.

The hippocampus plays a central role in learning and memory. Within the canonical trisynaptic hippocampal circuit, dentate gyrus granule cells (GCs) are first-station neurons that perform integration and coincidence detection of cortical inputs. This signal processing underlies pattern separation, a process critical to ensure that new memories are encoded separately from previous inputs (Jonas and Lisman, 2014). Tonic inhibition in dentate GCs plays a major role in these processes of neuronal signal filtering and integration (O'Neill and Sylantyev, 2018). We therefore used dentate gyrus GCs as a model system to probe whether and how FMRP regulates $GABA_AR$s to control tonic inhibition and signal integration in the hippocampus.

## RESULTS

### FMRP regulates single-channel activity of $GABA_ARs$

To investigate whether FMRP regulates $GABA_AR$ activity, we performed $GABA_AR$ single-channel recordings in outside-out patches excised from the somata of GCs of wild-type (WT) or *Fmr1* knockout (KO) mice. In the absence of exogenous GABA, we observed 3 open states (i.e., low-, mid- and high-conductance states) in both WT and KO mice (Figures 1A and 1B) (Yeung et al., 2003). We developed a Gaussian fit with subtraction method (Figure S1) and successfully isolated 3 open states and their corresponding single-channel properties. We found that loss of FMRP reduced single-channel currents/conductances in mid- and high-conductance states, with no significant changes in the low-conductance state (Figures 1C and 1D; statistical data for every measurement in this study are listed in Table S1). Furthermore, loss of FMRP decreased the $GABA_AR$ open probability in the high-conductance state and increased it in the low-conductance state, with no changes observed in the mid-conductance state (Figure 1E). Changes in open probability could be attributed to altered open frequency and/or open dwell time (open duration). We thus analyzed the $GABA_AR$'s open dynamics and found that loss of FMRP reduced open frequency in the high-conductance state, increased it in the low-conductance state, and had no effect in the mid-conductance state (Figure 2A). We further observed changes in open dwell time (Figures 2B–2D); specifically, loss of FMRP reduced open dwell times in the

high-conductance state, but increased it in low- and mid-conductance states (Figure 2F). We did not observe significant changes in the closed dwell time in the *Fmr1* KO GCs compared with WT GCs (Figures 2E and 2F).

To better understand the overall impact of these complex changes on $GABA_AR$ activity, we calculated the channel's weighted mean current/conductance and found that it was significantly decreased in *Fmr1* KO GCs compared with WT GCs (Figure 2G), indicating that the overall function of $GABA_ARs$ is decreased in KO GCs. We then determined the contributions of the 3 conductance states to the overall charge transfer by integrating conductances and their corresponding open probabilities (Figure 2H). This analysis showed that the contribution of the high-conductance state decreased in *Fmr1* KO GCs by ~61% while the contribution of the low-conductance state increased by ~48%, without a significant change in the mid-conductance state (Figure 2H).

Taken together, these results show that FMRP loss markedly alters $GABA_AR$ single-channel activity in GCs, causing an overall reduction of $GABA_AR$ function. This is evident in a redistribution of the receptor's open states in which conductance and open probability are decreased in the high-conductance state, while open probability is increased in the low-conductance state. We note that in addition to the relevance of these observations to FXS, these results also advance our understanding of $GABA_AR$ biophysics since, to the best of our knowledge, no native auxiliary regulators of $GABA_AR$ conductance have been previously reported in neurons.

## FMRP regulates spontaneous opening of extrasynaptic $GABA_ARs$ mediating tonic inhibition

The persistent activity of extrasynaptic $GABA_ARs$ is the core mechanism of tonic inhibition (Belelli et al., 2009; Bryson et al., 2020). Our observation that somatic $GABA_AR$ activity is decreased by FMRP loss thus predicts that tonic inhibition may also be reduced by FMRP loss. To examine this possibility, we performed whole-cell recordings in GCs and defined tonic inhibition as the difference in the holding current before and during application of picrotoxin (100 μM) (Wlodarczyk et al., 2013). As predicted, we found significantly reduced tonic inhibition in *Fmr1* KO GCs (Figures 3A and 3B). Tonic inhibition could arise from activation of $GABA_ARs$ by ambient GABA or from spontaneous openings of $GABA_ARs$ (Belelli et al., 2009). In the former case, it is possible that reduced tonic inhibition is caused by decreased ambient GABA concentrations in *Fmr1* KOs. To examine this possibility, we exogenously administered GABA (1, 3, or 10 μM) and then measured tonic inhibition. We found that, at the same GABA concentrations, tonic inhibition was still significantly reduced in *Fmr1* KO GCs compared with WT GCs (Figures 3A and 3B), and the extent of this reduction was nearly the same whether exogenous GABA was present (on average, 46.3%) or not (49.5%). Thus, the decreased tonic inhibition arises, in large part, from dysfunction of $GABA_ARs$ per se in *Fmr1* KO neurons rather than from insufficient ambient GABA concentrations.

We next evaluated to what extent the spontaneous opening of $GABA_ARs$ contributes to the reduction of tonic inhibition in *Fmr1* KOs. To isolate the GABA-independent (due to spontaneous opening of $GABA_ARs$) component of tonic inhibition, we took advantage of

the distinct properties of two $GABA_AR$ antagonists (gabazine versus picrotoxin): the effect of gabazine, as a competitive antagonist, is GABA-dependent, while picrotoxin blocks all $GABA_AR$ openings. Thus, in the presence of gabazine, the effect of picrotoxin is GABA-independent. We found that gabazine completely abolished spontaneous inhibitory postsynaptic currents but had no effect on the holding current (i.e., tonic inhibition) in both WT and KO neurons (Figures 3D and 3E), suggesting that GABA-dependent tonic inhibition in GCs is negligible in both genotypes. However, in the presence of gabazine, picrotoxin produced significantly smaller changes in holding current in *Fmr1* KO neurons (Figure 3E), indicating that GABA-independent tonic inhibition is decreased in KO neurons. Thus, both total tonic inhibition and GABA-independent tonic inhibition were strongly decreased in *Fmr1* KO neurons and to a similar extent (Figure 3F). These results show that FMRP regulates spontaneous $GABA_AR$ activity, which accounts for the vast majority of tonic inhibition in GCs.

$GABA_ARs$ have a pentameric structure composed of two α, two β, and one of either the β, γ, ε, θ, π, or ρ subunits. In GCs, δ-containing $GABA_ARs$ (δ-$GABA_ARs$) mediate a large proportion of tonic inhibition (Nusser and Mody, 2002). We thus tested to what extent dysfunction of δ-$GABA_ARs$ contribute to the decrease in tonic inhibition in *Fmr1* KO neurons by using a specific δ-$GABA_AR$ agonist THIP. The effect of THIP on tonic inhibition was markedly smaller in *Fmr1* KO than in WT neurons at all tested concentrations (Figure 3C), suggesting a reduced contribution from δ-$GABA_ARs$ in the KO neurons. Indeed, we estimated that loss of FMRP reduced tonic inhibition by 42.9% when evaluated by THIP, which constitute a large proportion of the overall reduction of 49.5%. This analysis indicates that the reduction of tonic inhibition is in a large part due to defects in δ-$GABA_ARs$ in *Fmr1* KO GCs.

## FMRP interacts with $GABA_A$ Rs

Given that FMRP rapidly and directly interacts with a number of ion channels to regulate their activity (Deng and Klyachko, 2021), we next asked whether FMRP interacts with $GABA_ARs$ to modulate tonic inhibition in GCs. If this is the case, we reasoned that acute neutralization of FMRP in WT GCs should mimic the reduced tonic inhibition observed in the KO neurons. Using a miniaturized perfusion system (Deng et al., 2019; Myrick et al., 2015), we applied a monoclonal antibody (Ab) (1:400) against the N-terminal part of FMRP via a patch pipette to acutely neutralize FMRP in the WT GCs. The Ab perfusion produced an outward shift of holding current (Figure 3G) and significantly reduced tonic inhibition in WT GCs (Figures 3G and 3H), indicating that acute neutralization of FMRP in WT GCs phenocopied the reduced tonic inhibition observed in KO GCs. To verify the specificity of the FMRP Ab, we performed the same experiments in the *Fmr1* KO mice. The Ab neither changed the holding current (Figure 3G) nor tonic inhibition (Figure 3H) in KO GCs, supporting that the FMRP Ab reduces tonic inhibition in WT neurons specifically by neutralizing FMRP.

The rapid effect of the FMRP Ab on tonic inhibition suggests that FMRP might directly interact with $GABA_ARs$ to regulate their activity and tonic inhibition. If this is the case, reintroduction of FMRP into the *Fmr1* KO neurons would be expected to rapidly

increase tonic inhibition. We tested this possibility by acutely perfusing the N-terminal FMRP fragment aa 1–297 ($FMRP_{297}$, 100 nM) in the KO GCs via a recording pipette and measuring changes in the holding current and tonic inhibition. We found that rapid introduction of $FMRP_{297}$ in the KO GCs produced an inward shift in the holding current (Figure 3I) and significantly increased tonic inhibition (Figures 3I and 3J) to the WT levels. The heat-inactivated $FMRP_{297}$ had no effect on the holding current or tonic inhibition (Figures 3I and 3J).

To further support the interaction between FMRP and $GABA_A$Rs, we used a biochemical approach to test whether FMRP interacts with any of the $GABA_A$R subunits commonly found in extrasynaptic $GABA_A$Rs in GCs: α4, α5, and δ (Farrant and Nusser, 2005). We observed a reliable co-immunoprecipitation (coIP) of the α5 subunit of $GABA_A$R with FMRP. Specifically, when the α5 subunit of $GABA_A$R was immunoprecipitated from brain lysate of WT mice, or from *Fmr1* KO mice as a negative control, and analyzed by western blot for FMRP, we observed coIP of the α5 subunit with FMRP in WT but not *Fmr1* KO mice (Figure 3K). We opted to IP with the $GABA_A$R α5-subunit Ab and probe for FMRP because in the reverse experiment, probing for the α5 subunit would not be interpretable due to the fact that the α5subunit of $GABA_A$R is around 55 kD, which is a similar molecular weight as the immunoglobulin G (IgG) heavy chain used for IP, and despite a crosslinking step, the IgG heavy chain is detected (Figure 3K). Western blot for GAPDH and ponceau staining (Figure 3K, bottom panel) confirmed that similar amount of input material was used for WT and *Fmr1* KO. These results suggest that FMRP interacts with the α5 subunit of $GABA_A$R. We cannot exclude the possibility that FMRP may also interact with other $GABA_A$R subunits such as a4 and δ, but due to the limitations of our coIP experiments, we could only reliably confirm interaction with the α5 subunit.

Taken together, these results support the notion that FMRP interacts with $GABA_A$Rs to rapidly regulate their activity and tonic inhibition in dentate gyrus GCs.

## FMRP regulates coincidence detection in dentate gyrus GCs

Coincidence detection is one of the critical mechanisms underlying pattern separation essential for successful memory storage and recall (Jonas and Lisman, 2014), and this process is regulated by GABAAR-mediated tonic inhibition (O'Neill and Sylantyev, 2018). We therefore examined the role of FMRP-$GABA_A$R interactions in coincidence detection in dentate gyrus GCs and its implications to information processing deficits in the absence of FMRP.

To measure the coincidence detection time window, two equal size excitatory postsynaptic current (EPSC)-like currents were injected via a recording pipette at different intervals (Δt from 0 to ± 40 ms; Figures 4A, 4B, and S2A) to evoke a pair of excitatory potentials (see STAR Methods for details). The amplitude of the input currents was gradually increased to reach ~50% probability to evoke a single action potential (AP) when two inputs were coincidental (δt = 0 ms), and this current intensity was fixed for the rest of the measurements in the same cell. Under these conditions, we found that the coincidence-detection time window was significantly broader in *Fmr1* KO neurons (Figure 4B). We also noticed that loss of FMRP increased excitability of GCs, as evident by the reduced AP threshold and

increased spiking (Figure S3). However, this did not affect our measurements of coincidence detection because stimulus intensity was set so that the AP firing probability did not differ at δt = 0 between genotypes (Table S1). To better understand the role of FMRP in regulating the coincidence-detection time window, we measured several key parameters that are known to correlate with the accuracy of coincidence detection, namely the excitatory potential summation ratio and decay time (Cook et al., 2003; Kuba et al., 2002) (Figure S2). Because we noticed a larger variability of AP timing in KO neurons (i.e., AP jitter; Figure 4A, insert), we also examined the top width of excitatory potential, which was defined as the width at 97.5% height of the 2nd peak of the excitatory potential (see STAR Methods for details) (Figure S2). We found that all these parameters were significantly increased in *Fmr1* KO neurons compared with WT neurons (Figure 4C), suggesting that a stronger and prolonged excitatory postsynaptic potential (EPSP) summation results in a wider coincidence-detection time window in the KO neurons. Together, these results indicate that FMRP can confine the coincidence-detection time window and regulate signal integration.

Tonic $GABA_AR$ conductance can act to reduce the amplitude and decay time of the membrane voltage changes through $GABA_AR$-driven hyperpolarization and shunting (Farrant and Nusser, 2005). Thus, the broadened coincidence-detection time window in *Fmr1* KO neurons could be caused by the reduced $GABA_AR$-mediated tonic inhibition. If this is the case, we reasoned that blocking spontaneous opening of $GABA_ARs$ should eliminate the differences in the coincidence-detection time window between genotypes. To examine this possibility, we first excluded the circuit effects of $GABA_AR$ inhibition on coincidence detection by pharmacologically isolating GCs with a cocktail of both glutamatergic and GABAergic antagonists (in μM, 50 APV, 10 DNQX, 10 MPEP, 5 gabazine, 2 CGP55845). We found that in the pharmacologically isolated GCs, the differences between genotypes in the coincidence-detection time window and excitatory potential parameters (Figures 4D and 4E) remain largely the same as those observed in the intact circuit (Figures 4B and 4C), indicating that the coincidence detection deficits in the *Fmr1* KO neurons have a cell-autonomous origin. Importantly, in isolated GCs, picrotoxin (100 mM) abolished the differences in the coincidence-detection time window, as well as in excitatory potential summation, top width, and decay time between genotypes (Figures 4F and 4G).

We note that similarly to deficits of coincidence detection in the absence of FMRP, increased excitability of GCs had a cell-autonomous origin (Figures S3A and S3B) and was also caused by reduced spontaneous opening of $GABA_ARs$ (Figures S3C, S3E, and S3F). In contrast, loss of FMRP had no effect on the passive membrane properties, including resting membrane potential, capacitance, and input resistance of GCs (Figures S4A–S4C), nor were the basal excitatory and inhibitory inputs onto GCs affected (Figures S4D–S4G).

Together, these results suggest that FMRP regulates activity of spontaneously opening $GABA_ARs$ to control excitability, tonic inhibition, and coincidence detection in GCs.

## DISCUSSION

Our results demonstrate that FMRP interacts with $GABA_A$Rs and regulates their activity at the single-channel level. The FMRP-$GABA_A$R interaction controls the spontaneous opening of the receptor by modulating its conductance and open probability. Physiologically, the FMRP-$GABA_A$R interaction regulates tonic inhibition to maintain neuronal excitability and ensure accurate signal integration and coincidence detection of dentate gyrus GCs. Consequently, loss of FMRP leads to dysregulation of this critical $GABA_A$R-dependent signaling, resulting in reduced single-channel activity of spontaneously opening $GABA_A$Rs, decreased tonic inhibition, and less-precise signal integration of GCs. The present study thus demonstrates that FMRP interacts with a neuronal receptor to regulate its activity. This interaction represents a molecular mechanism by which FMRP regulates important aspects of information processing in the dentate gyrus and advances our understanding of the pathophysiology of FXS.

### FMRP regulates $GABA_A$R single-channel activity

In FXS, the dysfunction of the GABAergic system, including both phasic and tonic inhibition, is believed to play major roles in the clinical phenotypes (Van der Aa and Kooy, 2020). Yet the mechanisms and physiological consequences of abnormal GABAergic inhibition in FXS remain poorly understood. While FMRP is well established to regulate translation of a large number of neuronal proteins, including over half of $GABA_A$R subunits (Van der Aa and Kooy, 2020), recent evidence shows that FMRP can also interact with several $K^+$ and $Ca^{2+}$ channels to rapidly regulate their activity directly (Brown et al., 2010; Deng et al., 2013, 2019; Yang et al., 2018; Zhan et al., 2020). Via these protein-protein interactions, FMRP controls neuronal excitability in many parts of the brain. However, whether this direct and rapid form of modulation by FMRP is limited to classical ion channels and cellular excitability, or has more widespread functions, has remained unknown.

In the present study, we demonstrate that FMRP regulates $GABA_A$R activity at the single-channel level. This includes modulation of single-channel conductance and open probability of $GABA_A$R. We further demonstrate that rapid neutralization of FMRP by an Ab against the N-terminal half of FMRP in WT neurons phenocopies reduction of tonic inhibition observed in *Fmr1* KO GCs. Moreover, acute reintroduction of the N-terminal $FMRP_{297}$ fragment (which is incapable of translational regulation) in *Fmr1* KO neurons is sufficient to normalize tonic inhibition to WT levels within minutes. The modulation of $GABA_A$R single-channel properties by FMRP together with the rapid and reversible actions of FMRP on tonic inhibition is consistent with protein-protein interactions of FMRP with $GABA_A$Rs. This interaction mechanism is further supported by our coIP experiments. Thus, our results provide evidence that FMRP can interact with a neuronal receptor to regulate its single-channel activity. Future studies will be needed to determine if this type of regulation is present in other brain areas and/or is limited to $GABA_A$Rs or also involves other neuronal receptors.

Native $GABA_A$Rs are heteropentamers, and the agonist/modulator binding sites in $GABA_A$Rs are located at inter- or intra-subunit interfaces. For example, neurosteroids enhance tonic inhibition mediated by δ-$GABA_A$Rs via two binding sites: one located at

the α-β subunit interface and the other within the α subunit (Stell et al., 2003). Similarly, our observation that dysfunction of δ-$GABA_A$Rs contribute significantly to reduced tonic inhibition in *Fmr1* KO neurons does not necessarily mean that FMRP directly interacts with the δ subunit. Indeed, our coIP analysis shows that FMRP interacts with the α5 subunit of $GABA_A$R. Importantly, our results do not exclude the possibility that FMRP also interacts with other $GABA_A$R subunits commonly involved in tonic inhibition, but it was not detected reliably in our coIP experiments. In fact, δ subunits often co-assemble with α4, and we observed FMRP interaction with α4 in some experiments (data not shown) but could not verify it robustly. Thus, these results only provide proof-of-principle evidence that FMRP interacts with at least one subunit of $GABA_A$R. A number of different $GABA_A$R compositions have been identified at extrasynaptic sites and capable of generating a tonic conductance in various brain regions (Brickley and Mody, 2012). Among these, α4βδ and α5βγ2 are most common, but α5βδ have also been suggested to function at extrasynaptic sites in the neocortex and hippocampus (Sperk et al., 2021; Brickley and Mody, 2012; Reddy, 2013). Thus, it remains to be determined whether α5-containing and δ-containing $GABA_A$Rs represent two different or the same population of $GABA_A$Rs contributing to reduced tonic inhibition in the absence of FMRP. More broadly, given that there is a large number of known subunit compositions of the $GABA_A$Rs, extensive future studies will be required to define which $GABA_A$R compositions interact with FMRP. Notably, our observation that, via this interaction, FMRP regulates $GABA_A$R conductance is also fundamentally significant for understanding $GABA_A$R regulation. While the subunit composition of the $GABA_A$R is known to affect single-channel conductance (Han et al., 2021), to the best of our knowledge, there are no other known auxiliary modifiers of $GABA_A$R conductance previously described.

Importantly, FMRP regulation of $GABA_A$Rs and tonic inhibition is an interplay of multiple mechanisms, which, in addition to protein-protein interactions reported here, include translational regulation and changes in receptor surface expression. This is evident in reduced expression levels of the $GABA_A$R δ subunit in several brain areas, including the dentate gyrus (Adusei et al., 2010; D'Hulst et al., 2009; D'Hulst et al., 2006; D'Hulst et al., 2015; Olmos-Serrano et al., 2010; Sabanov et al., 2017; Vien et al., 2015; Zhang et al., 2017), and reduced surface levels of the δ subunit reported in GCs (Zhang et al., 2017). In addition, reduced ambient GABA levels due to decreased glutamic acid decarboxylase (GAD) or reduced GABA release have been observed in *Fmr1* KO mice (Braat et al., 2015; Davidovic et al., 2011; Olmos-Serrano et al., 2010). These mechanisms also contribute to altered tonic inhibition, although they may play a less prominent role in the case of dentate GCs, in which tonic inhibition is largely GABA-independent (Wlodarczyk et al., 2013). Collectively, even though multiple mechanisms contribute to the modulation of tonic inhibition, our findings that tonic inhibition in *Fmr1* KO neurons can be rapidly normalized to WT levels in a translation-independent manner suggest that the FMRP-$GABA_A$R interaction plays a major role in the modulation of tonic inhibition in dentate GCs.

### FMRP-$GABA_A$R interaction and signal processing in the hippocampus

Coincidence detection in GCs is a critical mechanism for pattern separation of cortical inputs, which is essential for memory storage and recall (Cayco-Gajic and Silver, 2019).

This function requires GCs to maintain a narrow and precisely controlled coincidence-detection time window. Our results indicate that via the regulation of spontaneously opening $GABA_A$Rs, FMRP enhances tonic inhibition to sharpen coincidence detection. Consequently, loss of FMRP markedly deteriorates the accuracy of coincidence detection, which is phenocopied by blocking tonic inhibition in WT GCs.

Tonic inhibition can maintain the accuracy of coincidence detection via several concurrent mechanisms. Tonic $GABA_A$R conductance can work via its hyperpolarizing and shunting actions to reduce the amplitude and decay time of the membrane potential changes, which are two critical parameters determining the acuity of coincidence detection (Farrant and Nusser, 2005). In line with this mechanism, we found that reduced tonic inhibition in *Fmr1* KO GCs prolonged the decay time and top width of excitatory potentials, thus enhancing their summation and increasing variability of AP timing, which leads to a broadening of the coincidence-detection time window. In addition, tonic inhibition can also enhance accuracy of coincidence detection by setting the AP threshold (Azouz and Gray, 2000). Indeed, we found that the AP threshold is decreased in *Fmr1* KO GCs in a cell-autonomous manner and that blocking tonic inhibition eliminates the difference in AP threshold between genotypes.

In conclusion, our results demonstrate that FMRP interacts with extrasynaptic $GABA_A$Rs and regulates their activity to modulate signal integration and maintain accurate coincidence detection in the GCs. This interaction represents a mechanism by which FMRP regulates some of the critical aspects of signal processing in the hippocampus and thus advances our understanding of pathophysiology of FXS.

### Limitations of the study

The main conceptual limitation is that our current analyses are limited to one cell type and one brain area, while some of the effects of FMRP are known to be cell-type and brain-area specific. Moreover, electrophysiological recordings of native $GABA_A$Rs do not permit us to define the composition of the spontaneously opening $GABA_A$Rs regulated by FMRP, except for the predominance of the δ-$GABA_A$Rs. Thus, the conductance/gating changes observed in our single-channel recordings may not directly or fully reflect the activity of the same $GABA_A$Rs as those identified in coIP experiments or those involved in the signal integration in GCs. This limitation also partially arises from lack of cellular specificity of the coIP experiments, which cannot be performed from native GCs alone.

## STAR★METHODS

### RESOURCE AVAILABILITY

**Lead contact—**Further information and requests for resources and reagents should be directed to and will be fulfilled by the lead contact, Dr. Vitaly A. Klyachko (klyachko@wustl.edu).

**Material availability—**This study did not generate new or unique reagents or other materials.

### Data and code availability

- This paper does not report standardized data types. All data reported in this paper will be shared by the lead contact upon request.
- This paper does not report stand alone custom code. Labview, MATLAB, Origin and Mini analysis software packages were used to appropriately organize, process, and analyze data and corresponding routines are available from the lead contact upon request.
- Any additional information required to reanalyze the data reported in this paper is available from the lead contact upon request.

## EXPERIMENTAL MODEL AND SUBJECT DETAILS

**Animals and slice preparation—***Fmr1* KO (FVB.129P2-Pde6b$^{+}$ Tyr$^{c\text{-}ch}$ Fmr1$^{tm1Cgr}$/J; stock #004624) and WT control mice (FVB.129P2-Pde6b$^{+}$Tyr$^{c\text{-}ch}$/AntJ; stock #004828) were obtained from The Jackson Laboratory. Slices were prepared as previously described (Deng et al., 2019). In brief, male 21–23-day-old mice were used. After being deeply anesthetized with $CO_2$, mice were decapitated and their brains were dissected out in ice-cold saline containing the following (in mm): 130 NaCl, 24 $NaHCO_3$, 3.5 KCl, 1.25 $NaH_2PO_4$, 0.5 $CaCl_2$, 5.0 $MgCl_2$, and 10 glucose, pH 7.4 (saturated with 95% $O_2$ and 5% $CO_2$). Horizontal hippocampal slices (350 μm) were cut using a vibrating microtome (Leica VT1100 S) (Deng et al., 2019). Slices were initially incubated in the above solution at 35°C for 1 h for recovery and then kept at room temperature (~23°C) until use. All animal procedures were in compliance with the US National Institutes of Health Guide for the Care and Use of Laboratory Animals, and conformed to Washington University Animal Studies Committee guidelines.

## METHOD DETAILS

**Single channel recordings—**$GABA_AR$ single-channel recordings were performed in outside-out configuration at 33–34°C (temperature for all recordings in the present study) and voltage clamped at −80 mV using an Axopatch 700B (Molecular Devices) obtained from the somata of dentate gyrus GCs visually identified with infrared video microscopy and differential interference contrast optics (Olympus BX51WI). $GABA_AR$ single-channel activity was confirmed based on sensitivity to picrotoxin (PTX). Recordings were low-pass-filtered at 2 kHz and digitized at 20 kHz. To avoid recording from newly generated immature granule cells, we used cells located at the outer regions of the granule cell layer in the present study (Schmidt-Hieber et al., 2007). The recording pipette solution contained (in mM): 130 CsCl, 2 $MgCl_2$, 4 Mg-ATP, 0.3 Na-GTP, 10 HEPES, and 0.1 EGTA, 1 QX314 (Osmolarity 295 mOsm and pH 7.3). The extracellular solution contained the following (in mM): 125 NaCl, 24 $NaHCO_3$, 3.5 KCl, 1.25 $NaH_2PO_4$, 2 $CaCl_2$, 1 $MgCl_2$, and 10 glucose (pH 7.4, saturated with 95% $O_2$ and 5% $CO_2$).

**Tonic inhibition measurement—**Holding currents were recorded in the whole-cell mode (voltage clamped at −70 mV), using the same bath and pipette solutions as those in single channel recordings (for Figures 3A–3F). Holding current was defined by the center of Gaussian fit of all-point data distribution after digitally removing the spontaneous

postsynaptic currents. The tonic inhibition was defined as the difference (an outward shift) in holding currents between before and during application of picrotoxin (100 μM). Since we demonstrate that the most majority of tonic inhibition was mediated by spontaneously opening $GABA_A$Rs in GCs (Figure 3F), in order to maximally limit spontaneous postsynaptic currents contaminating holding current, in the following experiments (Figures 3G–3J) we used both glutamate and GABA receptors antagonists (in μM, 50 APV, 10 DNQX, 10 MPEP, 5 gabazine, 2 CGP55845) to block all postsynaptic currents and pharmacologically isolate the GCs.

**Determination of coincidence detection and excitatory potential summation**—Current-clamp recordings were made with bridge-balance compensation. The recording electrodes were filled with the following (in mM): 130 K-gluconate, 10 KCl, 0.1 EGTA, 2 $MgCl_2$, 2 $Na_2$-ATP, 0.4 Na-GTP, and 10 HEPES, pH 7.3. Coincidence detection was performed by injecting excitatory postsynaptic current (EPSC)-like stimulation (reversing the polarity of a previously recorded EPSC from WT GC, Figure S2A, low panel) to evoke excitatory potential (EP) via recording pipettes rather than using extracellular stimulation for two reasons: first, this allowed us to bypass the influence from the synaptic transmission observed in traditional coincidence detection experiments; second, EPSC-like current injected in the soma better represent the type of inputs that are involved in somatic integration in which tonic inhibition plays a critical role. Briefly, two equal size EPSC-like currents with different intervals (Δt=0,±2, ±4, ±6, ±10, ±15, ±20, ±25, ±30 and ±40 ms; Δt > 0, input 1 preceding input 2, and Δt < 0, input 1 following input 2) were injected from recording pipettes to evoke a pair of EPs. The amplitude of EPSC-like current was gradually increased to reach ~50% probability of a single action potential (AP) firing when two inputs were coincidental (Δt = 0 ms), and this current intensity was kept for the same cells. To better comparison among cells, the resting membrane potential of GCs was set to −80 mV (by constant current injection, if needed). Data were averaged over 10–15 trials for each cell and AP firing probabilities were normalized to that of Δt = 0 ms, which were then fitted by Gaussian function. The coincidence detection time window was defined as the half-height width of the Gaussian fit.

When the EPSC-like currents successfully triggered an AP, we also measured the AP jitter and voltage threshold. AP jitter (Figure 4A insert bar graph) was defined as the standard deviation of AP timing from the starting point of the 2nd EPSC-like current for each cell, and only APs at Δt = 0 ms were analyzed due to not having enough APs from a single cell to obtain reliable standard deviation at Δt ≠ 0 ms. AP threshold was defined as the voltage at the voltage trace turning point, corresponding to the first peak of 3rd order derivative of AP trace (Deng et al., 2019; Deng and Klyachko, 2016). Compared to AP firing timing, AP threshold is a relative stable parameter for a neuron in the same condition and thus relative less number of AP is needed, we then analyzed APs at Δt=0,±2, ±4, ±6 ms. When the EPSC-like currents failed to triggered an AP, we measured the summation ratio, top width and decay time of excitatory potentials (see supplemental information, Figure S2). Top width was defined as the width at 97.5% level of the 2nd excitatory potential peak (h2 in Figure S2), because all APs were triggered within this time window in coincidence detection experiments.

**Recording of ramp currents-evoked action potentials—**The recording conditions of ramp current-evoked AP were the same as those in coincidence detection experiments, except that action potentials were evoked by a ramp-current injection (increasing rate 0.05 pA/ms, Figure S3D, lower panel) with a hyperpolarizing onset. The AP threshold was determined only from the first APs to avoid the influence of cumulatively inactivating voltage-gated ion channels in the threshold of following APs. All data were averaged over 5–8 trials for each cell.

**Measurement of resting membrane potential, capacitance and input resistance—**Resting membrane potential (RMP) was measured immediately after whole-cell formation. Cell capacitance is determined by the amplifier's auto whole-cell compensation function with slightly manual adjustment to optimize the measurement if needed. Under current-clamp mode, a negative current (−50 pA for 500 ms) was injected every 5 s to assess the input resistance.

**Recordings of spontaneous and miniature postsynaptic currents—**Spontaneous excitatory postsynaptic currents (sEPSCs) were recorded from granule cells holding at −70 mV. The pipette solution was the same as that used in coincidence detection experiments, except that QX-314 (1 mM) was included in the pipette solution to block possible action current. The bath solution was supplemented with gabazine (5 μM) to block $GABA_AR$ responses. The solutions used to recording of miniature excitatory postsynaptic currents (mEPSCs) were the same as those for sEPSCs, except that tetrodotoxin (TTX, 1 μM) was included in the external solution to block action potential-dependent responses.

For recording of spontaneous inhibitory postsynaptic currents (sIPSCs), the recording conditions (including pipette and bath solutions) were the same as those used in tonic inhibition experiments, except that the bath solution was supplemented with APV (50 μM) and DNQX (10 μM) to block responses of ionotropic glutamate receptors. For miniature inhibitory postsynaptic currents (mIPSCs) recording, TTX was added in the bath solution.

**Co-immunoprecipitation experiments—**Mice were euthanized and perfused with ice cold phosphate buffer (PBS). Whole brain was collected and immediately homogenized on ice in lysis buffer (50 mM HEPES, pH 7.4, 150 mM NaCl, 1% Triton X-100, plus protease inhibitor/phosphatase inhibitor). Homogenized brain incubated on ice for 30 min was clarified by centrifugation at 14,500 rpm and protein concentration was measured by BCA assay kit. For the covalent cross-linking of the IgG antibody to protein A/G beads, the Abcam protocol was followed. In brief, 40 μL protein A/G magnetic beads were washed with PBS and rotated with PBS over night at 4°C. The supernatant was then discarded and beads were resuspended in dilution buffer (BSA 1 mg/mL in PBS) for 10 min. The supernatant was then discarded and dilution buffer containing 5 mg of anti-$GABA_AR$ α5 subunit antibody or IgG control was added and beads were incubated at 4°C for 2 h. After washing with wash buffer (0.2 M triethanolamine in PBS pH 8–9), 200 μL of cross-linking reagent (Dimethyl pimelimidate 6.5 mg/mL) was added in wash buffer and beads were incubated at room temperature on a rotator for 45 min. Beads were then washed with washing buffer and the cross-linking steps repeated once more. After two cycles of cross-linking the reaction was stopped with quenching buffer (50 mM ethanolamine in PBS).

To remove unbound antibodies, beads were incubated with 1 M glycine pH 2–3 for 10 min. Cross-linked beads were washed in lysis buffer and incubated with 1500 μg brain lysate overnight at 4°C. Beads were washed five times with lysis buffer before elution of bound proteins with 2X SDS/PAGE loading buffer. The immunoprecipitated material was analyzed by Western blot with anti-FMRP antibody and anti-GAPDH.

### QUANTIFICATION AND STATISTICAL ANALYSIS

The single channel recordings, tonic inhibition, coincidence detection and AP data were analyzed in MatLab. The postsynaptic currents (sEPSC, mEPSC, sIPSC and mIPSC) were analyzed by Mini Analysis. All figures were made in Origin or MatLab. Data are presented as mean ± SEM. Student's t test, one-way ANOVA or Kolmogorov–Smirnov (K-S) test were used for statistical analysis as appropriate. Significance was set as $p < 0.05$. The n in electrophysiological experiments was number of cells tested, which was from at least 3 different mice for each condition. The N in Co-IP experiments is number of animals used. All n and p values can be found in Table S1.

## Supplementary Material

Refer to Web version on PubMed Central for supplementary material.

## ACKNOWLEDGMENTS

This work was supported in part by NIH grant R35 NS111596 to V.A.K. and R01 NS111719 and R35 NS122260 to V.C. The Figure 4A diagram and the graphical abstract were created with BioRender.com.

## REFERENCES

Adusei DC, Pacey LK, Chen D, and Hampson DR (2010). Early developmental alterations in GABAergic protein expression in fragile X knockout mice. Neuropharmacol 59, 167–171. 10.1016/j.neuropharm.2010.05.002.

Azouz R, and Gray CM (2000). Dynamic spike threshold reveals a mechanism for synaptic coincidence detection in cortical neurons in vivo. Proc. Nat. Acad. Sci. U S A. 97, 8110–8115. 10.1073/pnas.130200797.

Belelli D, Harrison NL, Maguire J, Macdonald RL, Walker MC, and Cope DW (2009). Extrasynaptic GABAA receptors: form, pharmacology, and function. J. Neurosci. 29, 12757–12763. 10.1523/jneurosci.3340-09.2009. [PubMed: 19828786]

Braat S, D'Hulst C, Heulens I, De Rubeis S, Mientjes E, Nelson DL, Willemsen R, Bagni C, Van Dam D, De Deyn PP, and Kooy RF (2015). The GABAA receptor is an FMRP target with therapeutic potential in fragile X syndrome. Cell Cycle 14, 2985–2995. 10.4161/15384101.2014.989114. [PubMed: 25790165]

Brickley SG, and Mody I (2012). Extrasynaptic GABA(A) receptors: their function in the CNS and implications for disease. Neuron 73, 23–34. 10.1016/j.neuron.2011.12.012. [PubMed: 22243744]

Brown MR, Kronengold J, Gazula VR, Chen Y, Strumbos JG, Sigworth FJ, Navaratnam D, and Kaczmarek LK (2010). Fragile X mental retardation protein controls gating of the sodium-activated potassium channel Slack. Nat. Neurosci. 13, 819–821. 10.1038/nn.2563. [PubMed: 20512134]

Bryson A, Hatch RJ, Zandt BJ, Rossert C, Berkovic SF, Reid CA, Grayden DB, Hill SL, and Petrou S (2020). GABA-mediated tonic inhibition differentially modulates gain in functional subtypes of cortical interneurons. Proc. Nat. Acad. Sci. U S A 117, 3192–3202. 10.1073/pnas.1906369117.

Cayco-Gajic NA, and Silver RA (2019). Re-evaluating circuit mechanisms underlying pattern separation. Neuron 101, 584–602. 10.1016/j.neuron.2019.01.044. [PubMed: 30790539]

Cook DL, Schwindt PC, Grande LA, and Spain WJ (2003). Synaptic depression in the localization of sound. Nature 421, 66–70. [PubMed: 12511955]

Curia G, Papouin T, Seguela P, and Avoli M (2009). Downregulation of tonic GABAergic inhibition in a mouse model of fragile X syndrome. Cereb. Cortex 19, 1515–1520. 10.1093/cercor/bhn159. [PubMed: 18787232]

Davidovic L, Navratil V, Bonaccorso CM, Catania MV, Bardoni B, and Dumas ME (2011). A metabolomic and systems biology perspective on the brain of the fragile X syndrome mouse model. Genome Res. 21, 2190–2202. 10.1101/gr.116764.110. [PubMed: 21900387]

D'Hulst C, Atack JR, and Kooy RF (2009). The complexity of the GABAA receptor shapes unique pharmacological profiles. Drug Discov. Today 14, 866–875. 10.1016/j.drudis.2009.06.009. [PubMed: 19576998]

D'Hulst C, De Geest N, Reeve SP, Van Dam D, De Deyn PP, Hassan BA, and Kooy RF (2006). Decreased expression of the GABAA receptor in fragile X syndrome. Brain Res. 1121, 238–245. 10.1016/j.brainres.2006.08.115. [PubMed: 17046729]

D'Hulst C, Heulens I, Van der Aa N, Goffin K, Koole M, Porke K, Van De Velde M, Rooms L, Van Paesschen W, Van Esch H, et al. (2015). Positron emission tomography (PET) quantification of GABAA receptors in the brain of fragile X patients. PLoS One 10, e0131486. 10.1371/journal.pone.0131486. [PubMed: 26222316]

Deng PY, Carlin D, Oh YM, Myrick LK, Warren ST, Cavalli V, and Klyachko VA (2019). Voltage-independent SK-channel dysfunction causes neuronal hyperexcitability in the Hippocampus of Fmr1 knock-out mice. J. Neurosci. 39, 28–43. 10.1523/jneurosci.1593-18.2018. [PubMed: 30389838]

Deng PY, and Klyachko VA (2016). Increased persistent sodium current causes neuronal hyperexcitability in the entorhinal cortex of Fmr1 knockout mice. Cell Rep. 16, 3157–3166. 10.1016/j.celrep.2016.08.046. [PubMed: 27653682]

Deng PY, and Klyachko VA (2021). Channelopathies in fragile X syndrome. Nat. Rev. Neurosci. 22, 275–289. 10.1038/s41583-02100445-9. [PubMed: 33828309]

Deng PY, Rotman Z, Blundon JA, Cho Y, Cui J, Cavalli V, Zakharenko SS, and Klyachko VA (2013). FMRP regulates neurotransmitter release and synaptic information transmission by modulating action potential duration via BK channels. Neuron 77, 696–711. 10.1016/j.neuron.2012.12.018. [PubMed: 23439122]

Farrant M, and Nusser Z (2005). Variations on an inhibitory theme: phasic and tonic activation of GABA(A) receptors. Nat. Rev. Neurosci. 6, 215–229. 10.1038/nrn1625. [PubMed: 15738957]

Han W, Shepard RD, and Lu W (2021). Regulation of GABAARs by transmembrane accessory proteins. Trends Neurosci. 44, 152–165. 10.1016/j.tins.2020.10.011. [PubMed: 33234346]

Jonas P, and Lisman J (2014). Structure, function, and plasticity of hippocampal dentate gyrus microcircuits. Front Neural Circuits 8, 107. 10.3389/fncir.2014.00107. [PubMed: 25309334]

Kasugai Y, Swinny JD, Roberts JDB, Dalezios Y, Fukazawa Y, Sie-ghart W, Shigemoto R, and Somogyi P (2010). Quantitative localisation of synaptic and extrasynaptic GABAA receptor subunits on hippocampal pyramidal cells by freeze-fracture replica immunolabelling. Euro J. Neurosci. 32, 1868–1888. 10.1111/j.1460-9568.2010.07473.x.

Kuba H, Koyano K, and Ohmori H (2002). Synaptic depression improves coincidence detection in the nucleus laminaris in brainstem slices of the chick embryo. Eur. J. Neurosci. 15, 984–990. 10.1046/j.1460-9568.2002.01933.x. [PubMed: 11918658]

Lozano R, Hare EB, and Hagerman RJ (2014). Modulation of the GABAergic pathway for the treatment of fragile X syndrome. Neuropsychiatr. Dis. Treat. 10, 1769–1779. 10.2147/ndt.s42919. [PubMed: 25258535]

Martin BS, Corbin JG, and Huntsman MM (2014). Deficient tonic GABAergic conductance and synaptic balance in the fragile X syndrome amygdala. J. Neurophysiol. 112, 890–902. 10.1152/jn.00597.2013. [PubMed: 24848467]

Modgil A, Vien TN, Ackley MA, Doherty JJ, Moss SJ, and Davies PA (2019). Neuroactive steroids reverse tonic inhibitory deficits in fragile X syndrome mouse model. Front Mol. Neurosci. 12, 15. 10.3389/fnmol.2019.00015. [PubMed: 30804752]

Myrick LK, Deng PY, Hashimoto H, Oh YM, Cho Y, Poidevin MJ, Suhl JA, Visootsak J, Cavalli V, Jin P, et al. (2015). Independent role for presynaptic FMRP revealed by an FMR1 missense mutation associated with intellectual disability and seizures. Proc. Nat. Acad. Sci. U S A. 112, 949–956. 10.1073/pnas.1423094112.

Nusser Z, and Mody I (2002). Selective modulation of tonic and phasic inhibitions in dentate gyrus granule cells. J. Neurophysiol. 87, 2624–2628. 10.1152/jn.2002.87.5.2624. [PubMed: 11976398]

O'Neill N, and Sylantyev S (2018). Spontaneously opening GABAA receptors play a significant role in neuronal signal filtering and integration. Cell Death Dis. 9, 813. 10.1038/s41419-018-0856-7. [PubMed: 30042389]

Olmos-Serrano JL, Corbin JG, and Burns MP (2011). The GABA(A) receptor agonist THIP ameliorates specific behavioral deficits in the mouse model of fragile X syndrome. Develop Neurosci. 33, 395–403. 10.1159/000332884.

Olmos-Serrano JL, Paluszkiewicz SM, Martin BS, Kaufmann WE, Corbin JG, and Huntsman MM (2010). Defective GABAergic neurotransmission and pharmacological rescue of neuronal hyperexcitability in the amygdala in a mouse model of fragile X syndrome. J. Neurosci. 30, 9929–9938. 10.1523/jneurosci.1714-10.2010. [PubMed: 20660275]

Reddy DS (2013). Role of hormones and neurosteroids in epileptogenesis. Front Cell Neurosci. 7, 115. 10.3389/fncel.2013.00115. [PubMed: 23914154]

Sabanov V, Braat S, D'Andrea L, Willemsen R, Zeidler S, Rooms L, Bagni C, Kooy RF, and Balschun D (2017). Impaired GABAergic inhibition in the hippocampus of Fmr1 knockout mice. Neuropharmacol 116, 71–81. 10.1016/j.neuropharm.2016.12.010.

Salcedo-Arellano MJ, Dufour B, McLennan Y, Martinez-Cerdeno V, and Hagerman R (2020). Fragile X syndrome and associated disorders: clinical aspects and pathology. Neurobiol. Dis. 136, 104740. 10.1016/j.nbd.2020.104740. [PubMed: 31927143]

Schmidt-Hieber C, Jonas P, and Bischofberger J (2007). Subthreshold dendritic signal processing and coincidence detection in dentate gyrus granule cells. J. Neurosci. 27, 8430–8441. 10.1523/jneurosci.1787-07.2007. [PubMed: 17670990]

Stell BM, Brickley SG, Tang CY, Farrant M, and Mody I (2003). Neuroactive steroids reduce neuronal excitability by selectively enhancing tonic inhibition mediated by delta subunit-containing GABAA receptors. Proc. Nat. Acad. Sci. U S A. 100, 14439–14444. 10.1073/pnas.2435457100.

Sperk G, Pirker S, Gasser E, Wieselthaler A, Bukovac A, Kuchukhidze G, Maier H, Drexel M, Baumgartner C, Ortler M, and Czech T (2021). Increased expression of GABAA receptor subunits associated with tonic inhibition in patients with temporal lobe epilepsy. Brain Commun. 3, fcab239. 10.1093/braincomms/fcab239. [PubMed: 34708207]

Tang X, Jaenisch R, and Sur M (2021). The role of GABAergic signalling in neurodevelopmental disorders. Nat. Rev. Neurosci. 22, 290–307. 10.1038/s41583-021-00443-x. [PubMed: 33772226]

Van der Aa N, and Kooy RF (2020). GABAergic abnormalities in the fragile X syndrome. Eur. J. Paed Neurol. 24, 100–104. 10.1016/j.ejpn.2019.12.022.

Vien TN, Modgil A, Abramian AM, Jurd R, Walker J, Brandon NJ, Terunuma M, Rudolph U, Maguire J, Davies PA, and Moss SJ (2015). Compromising the phosphodependent regulation of the $GABA_AR$ β3 subunit reproduces the core phenotypes of autism spectrum disorders. Proc. Nat. Acad. Sci. U S A 112, 14805–14810. 10.1073/pnas.1514657112.

Whissell PD, Lecker I, Wang DS, Yu J, and Orser BA (2015). Altered expression of dGABAA receptors in health and disease. Neuropharmacol 88, 24–35. 10.1016/j.neuropharm.2014.08.003.

Wlodarczyk AI, Sylantyev S, Herd MB, Kersante F, Lambert JJ, Rusakov DA, Linthorst ACE, Semyanov A, Belelli D, Pavlov I, and Walker MC (2013). GABA-independent GABAA receptor openings maintain tonic currents. J. Neurosci. 33, 3905–3914. 10.1523/jneurosci.4193-12.2013. [PubMed: 23447601]

Yang YM, Arsenault J, Bah A, Krzeminski M, Fekete A, Chao OY, Pacey LK, Wang A, Forman-Kay J, Hampson DR, et al. (2018). Identification of a molecular locus for normalizing dysregulated GABA release from interneurons in the Fragile X brain. Mol. Psychiatry 25, 2017–2035. 10.1038/s41380-018-0240-0. [PubMed: 30224722]

Yeung JYT, Canning KJ, Zhu G, Pennefather P, MacDonald JF, and Orser BA (2003). Tonically activated GABAA receptors in hippocampal neurons are high-affinity, low-conductance sensors for extracellular GABA. Mol. Pharmacol. 63, 2–8. 10.1124/mol.63.1.2. [PubMed: 12488530]

Zhan X, Asmara H, Cheng N, Sahu G, Sanchez E, Zhang FX, Zamponi GW, Rho JM, and Turner RW (2020). FMRP(1–297)-tat restores ion channel and synaptic function in a model of Fragile X syndrome. Nat. Commun. 11, 2755. 10.1038/s41467-020-16250-4. [PubMed: 32488011]

Zhang N, Peng Z, Tong X, Lindemeyer AK, Cetina Y, Huang CS, Olsen RW, Otis TS, and Houser CR (2017). Decreased surface expression of the delta subunit of the GABAA receptor contributes to reduced tonic inhibition in dentate granule cells in a mouse model of fragile X syndrome. Exp. Neurol. 297, 168–178. 10.1016/j.expneurol.2017.08.008. [PubMed: 28822839]

## Highlights

- FMRP regulates single-channel activity of $GABA_AR$ in dentate granule cells (GCs)
- FMRP interacts with at least one $GABA_AR$ subunit, the α5
- FMRP-$GABA_AR$ interaction regulates tonic inhibition and excitability of dentate GCs
- FMRP-$GABA_AR$ interaction controls coincidence detection of dentate GCs

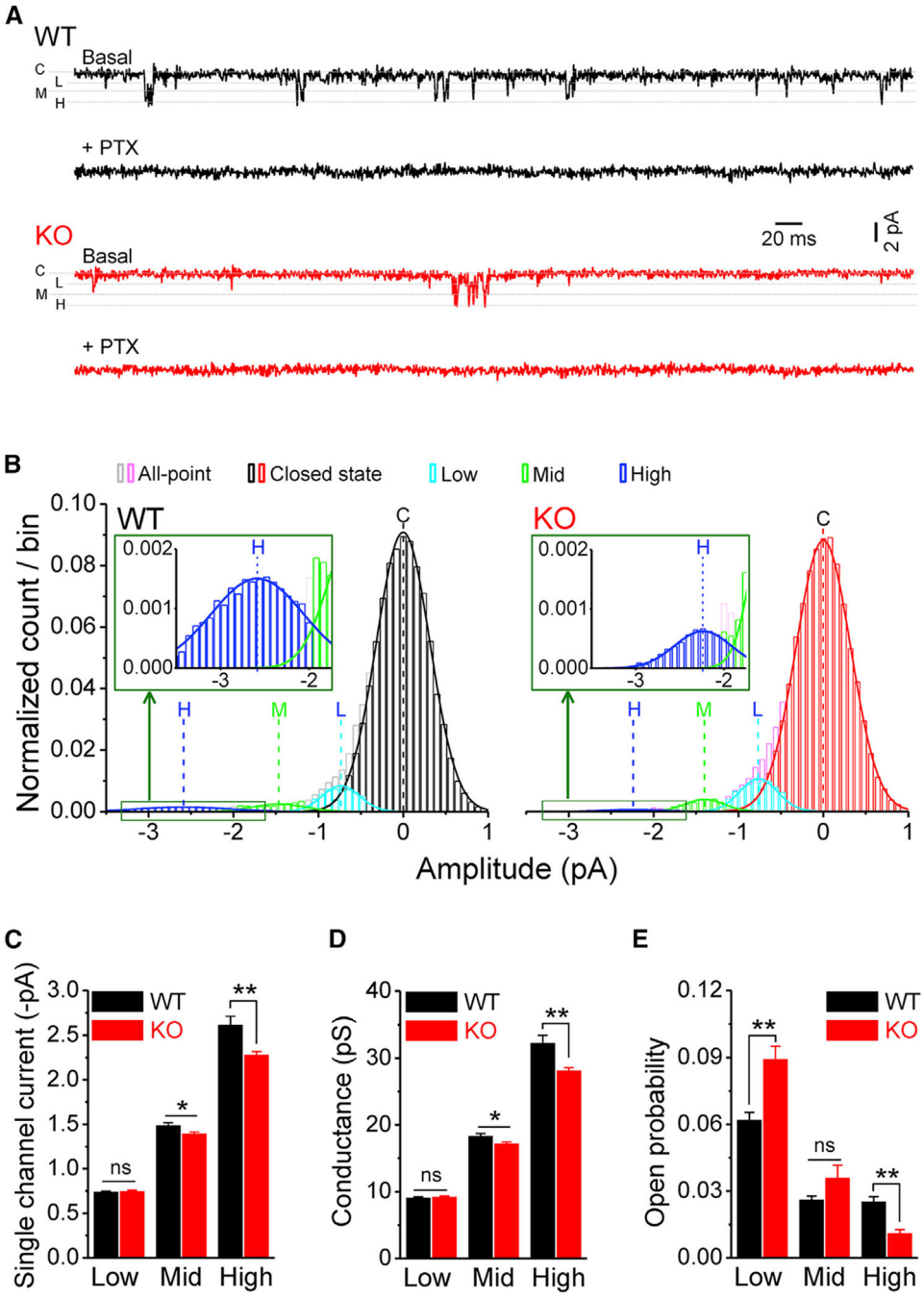


**Figure 1. Loss of FMRP affects $GABA_AR$ single-channel properties**

(A) Sample traces of $GABA_AR$ single-channel recordings in outside-out patches from dentate gyrus GCs in WT (black) and *Fmr1* KO (red). Line C denotes a closed state; lines L, M, and H are low-, mid- and high-conductance states, respectively. Note that picrotoxin (PTX) completely blocked all openings.

(B) All-point distribution of single-channel recordings and isolation of 3 open states using Gaussian fit with subtraction method (see Figure S1). Lines C, L, M, and H denote centers of Gaussian fits of closed, low- (cyan), mid- (green), and high- (blue) conductance

states, respectively. Inserts, enlargements of high-conductance states. For comparison among patches, the number of data points per bin was normalized to the corresponding total data points.

(C and D) Summarized data of single-channel currents (C) and conductances (D) of $GABA_A$Rs' low-, mid-, and high-conductance states.

(E) Open probability of $GABA_A$R's low-, mid-, and high-conductance states.

*p < 0.05; **p < 0.01; ns, not significant. The statistical data are listed in Table S1. Data are mean ± SEM.

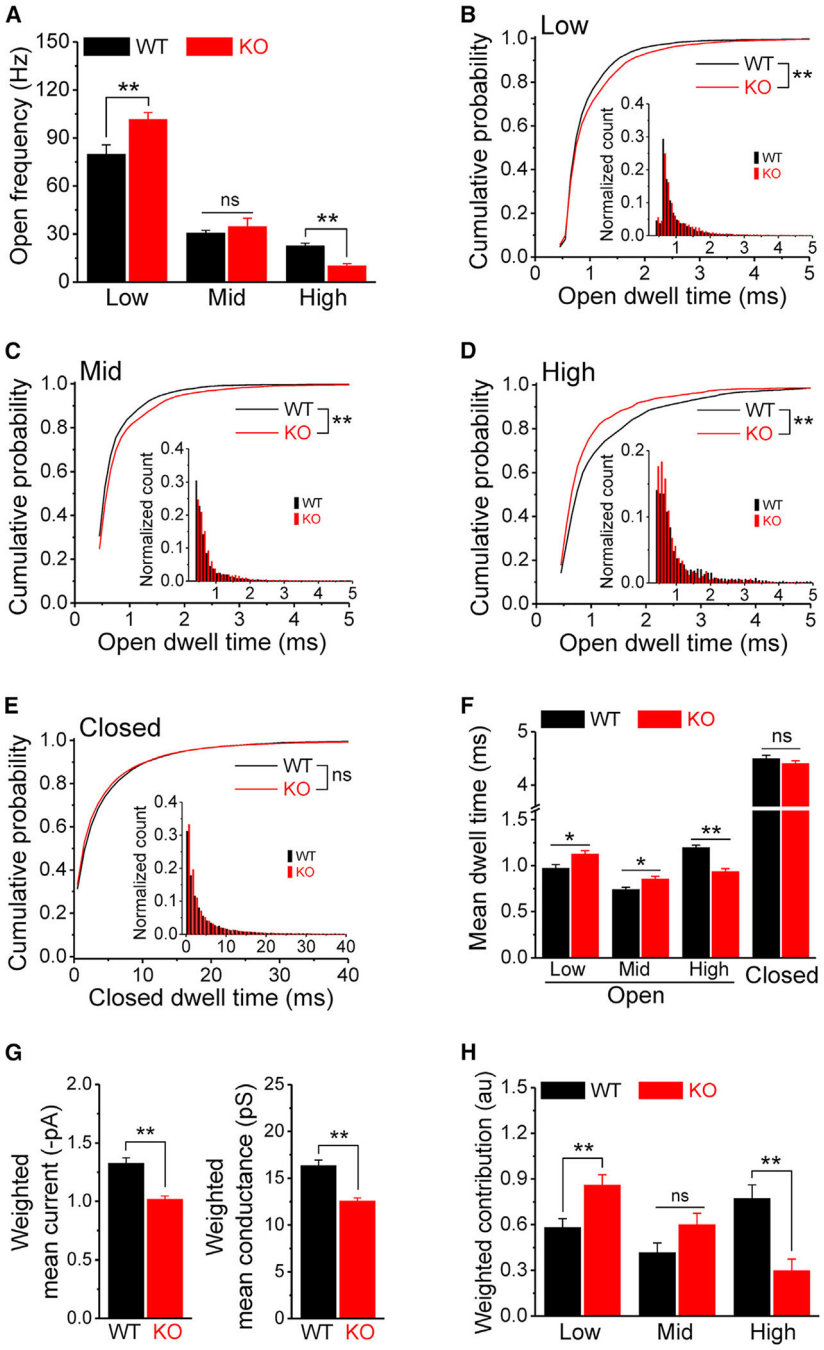


**Figure 2. Loss of FMRP alters GABA$_A$R open dynamics**

(A) Open frequency of GABA$_A$R's low-, mid-, and high-conductance states in WT and *Fmr1* KO.

(B–E) Cumulative probability of GABA$_A$R open dwell time for low- (B), mid- (C), and high- (D) conductance states and for closed dwell time (E). Insets, open (B–D, bin size = 0.1 ms) or closed (E, bin size = 1 ms) dwell-time distributions of corresponding states.

(F) Summarized data of dwell time for low-, mid-, and high-conductance and closed states.

(G) Weighted GABA$_A$R mean current and conductance in WT and *Fmr1* KO.

(H) Weighted contributions of 3 conductance states to $GABA_AR$ channel charge transfer. *p < 0.05; **p < 0.01; ns, not significant. The statistical data are listed in Table S1. Data are means ± SEM.

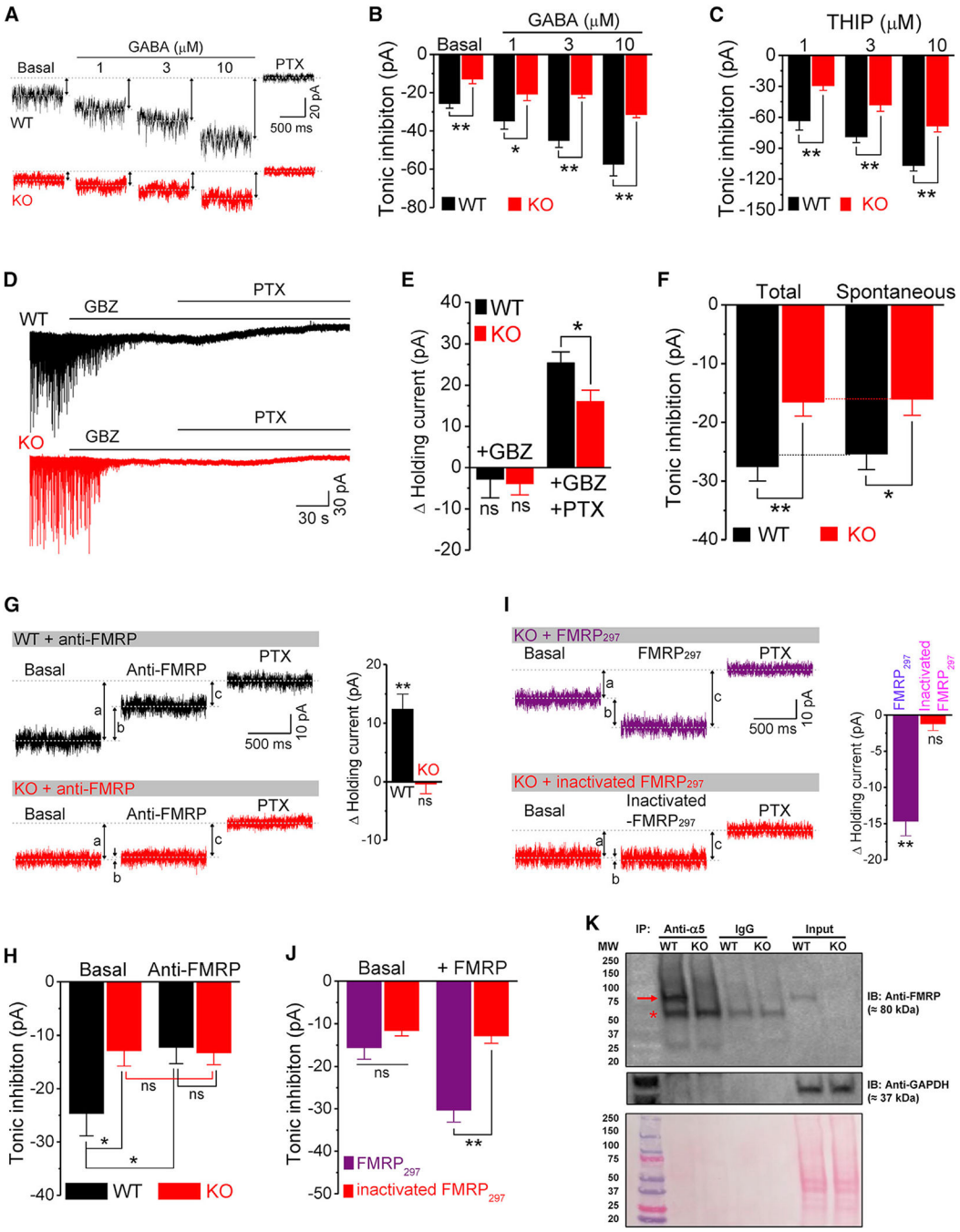


**Figure 3. FMRP interacts with GABA$_A$Rs to control GABA-independent tonic inhibition**

(A) Sample traces of tonic inhibition in basal condition and in response to exogenous application of GABA. Up-down arrows indicate amplitude of tonic inhibition. Postsynaptic currents were digitally removed for clarity.

(B) Summarized data of tonic inhibition in the basal condition and in response to exogenous application of GABA.

(C) Tonic inhibition in response to δ-GABA$_A$R-specific agonist THIP.

(D and E) Sample traces (D) and summarized data (E) of holding current in response to gabazine (GBZ) and PTX.

(F) Summarized data of total and spontaneous tonic inhibition.

(G and H) Sample traces (G) and summarized data (H) for the effects of FMRP antibody (anti-FMRP) on holding current and tonic inhibition. *a*, basal tonic inhibition (before application of anti-FMRP); *b*, effects of anti-FMRP on holding current; *c*, tonic inhibition in the presence of anti-FMRP. Bar graph in (G) shows effects of FMRP antibody on changes in holding current (i.e., *b* values). **p < 0.01; ns, not significant, versus Δ holding current = 0.

(I and J) Same as (G) and (H) for the effects of $FMRP_{297}$ and heat-inactivated $FMRP_{297}$ in *Fmr1* KO GCs.

(K) $GABA_AR$ α5 subunit was immunoprecipitated from protein extract prepared from WT or *Fmr1* KO mice brain and analyzed by western blot with anti-FMRP antibody. GAPDH was used as a loading control for the lysate and as a negative control for the IP. Bottom panel shows ponceau staining, which was used as an additional loading control for the lysate. Arrow: FMRP band; asterisk: IgG heavy-chain band. N = 4 independent coIP experiments for WT, N = 2 for *Fmr1* KO.

*p < 0.05; **p < 0.01; ns, not significant. The statistical data are listed in Table S1. Data are mean ± SEM.

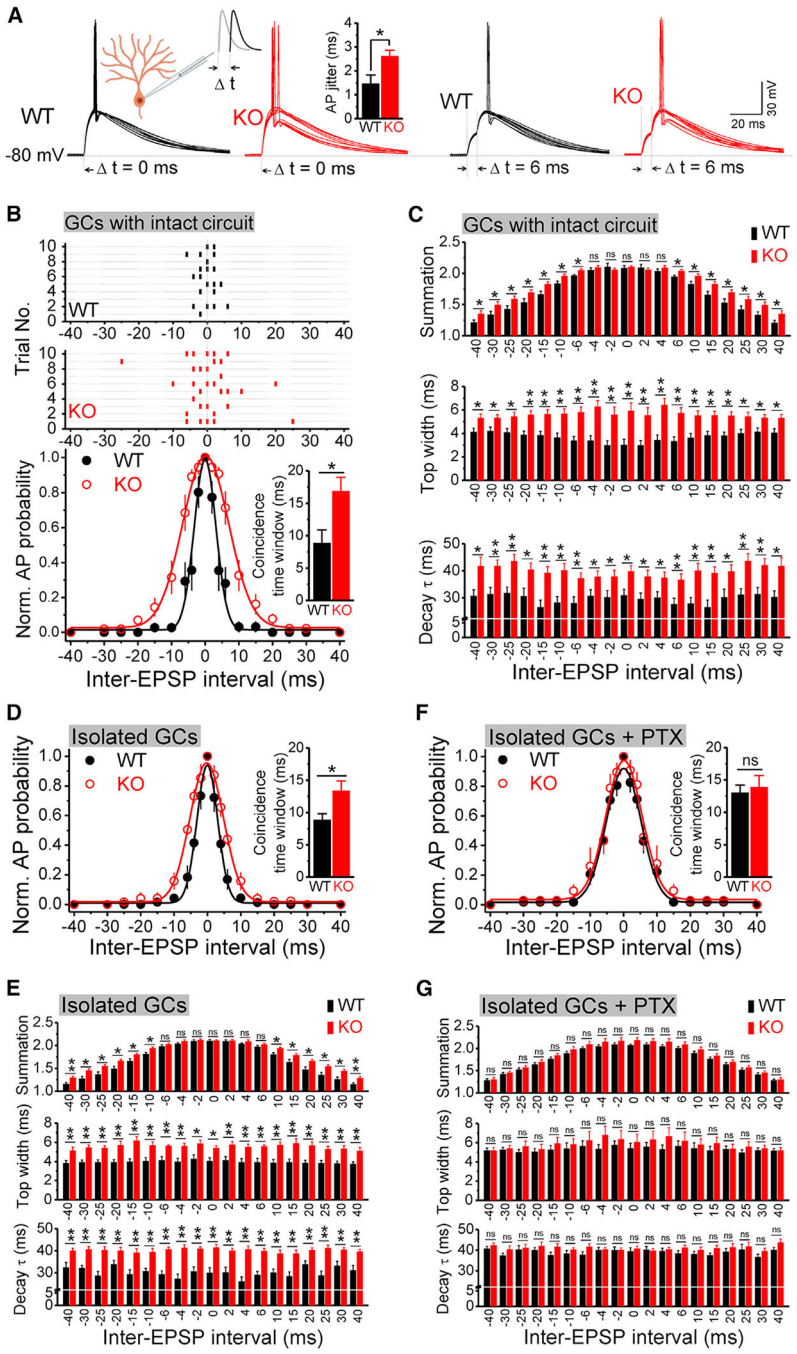


**Figure 4. FMRP regulates coincidence detection in dentate gyrus GCs**

(A) Sample traces of coincidence-detection measurements in WT and *Fmr1* KO GCs (10 trials overlapped for each panel). A pair of EPSC-like currents were injected via recording pipettes. Left insert, recording diagram; input 1 is in gray, and input 2 is in black, with inter-stimulus intervals δt from −40 to 40 ms, as shown in (C). Right insert, bar graph showing large AP jitter in KO GCs.

(B) Top panel, raster plot of AP firing (horizontal lines represent trials; ticks denote APs). Bottom panel, summarized data of coincidence-detection measurements fitted by Gaussian function. Insert, coincidence-detection time window.
(C) Analysis of excitatory potential summation ratio (top), top width (middle) and decay time constant (bottom) when injecting currents failed to trigger an AP.
(D) Same as in bottom panel of (B) but recorded from the pharmacologically isolated GCs.
(E) Same as (C) but recorded from the pharmacologically isolated GCs.
(F) Same as (D) but in the presence of PTX recorded from the pharmacologically isolated GCs.
(G) Same as (E) but in the presence of PTX recorded from the pharmacologically isolated GCs.
*$p < 0.05$; **$p < 0.01$; ns, not significant. The statistical data are listed in Table S1. Data are means ± SEM.

## KEY RESOURCES TABLE

| REAGENT OR RESOURCE | SOURCE | IDENTIFIER |
|---|---|---|
| Antibodies | | |
| Anti-FMRP antibody (for intracellular perfusion) | Millipore | Cat# MAB2160; RRID: AB_2283007 |
| Anti-FMRP antibody (for Co-Immunoprecipitation) | Cell Signaling Technology | Cat# 4317; RRID: AB_1903978 |
| Anti-GABAR α5 subunit antibody | Synaptic Systems | Cat# 224503; RRID: AB_2619944 |
| Anti-GAPDH | Santa Cruz Biotechnology | Cat# sc-25778; RRID: AB_10167668 |
| Chemicals, peptides, and recombinant proteins | | |
| (2 *S*)-3-[[(1 *S*)-1-(3,4-Dichlorophenyl)ethyl]amino-2-hydroxypropyl] (phenylmethyl)phosphinic acid hydrochloride (CGP55845) | Tocris Bioscience | 1248 |
| 4-(2-Hydroxyethyl)piperazine-1-ethanesulfonic acid, N-(2-Hydroxyethyl)piperazine-N′-(2-ethanesulfonic acid) (HEPES) | MilliporeSigma | H3375 |
| 4,5,6,7-Tetrahydroisoxazolo[5,4-c]pyridin-3-ol hydrochloride (THIP) | Tocris Bioscience | 0807 |
| 6,7-Dinitroquinoxaline-2,3-dione(DNQX) | Tocris Bioscience | 2312 |
| A/G magnetic beads | Thermo Scientific | 88803 |
| Adenosine 5'-triphosphate disodium ($Na_2$-ATP) | MilliporeSigma | A1852 |
| Adenosine 5'-triphosphate magnesium (Mg-ATP) | MilliporeSigma | A9187 |
| BCA assay kit | Thermo Scientific | 23227 |
| D-(-)-2-Amino-5-phosphonopentanoic acid (APV) | Tocris Bioscience | 0106 |
| Fragile X mental retardation protein aa1-297 ($FMRP_{297}$) | Novus Biologicals | H00002332-P01 |
| Guanosine 5′-triphosphate sodium (Na-GTP) | MilliporeSigma | G8877 |
| Picrotoxin (PTX) | Tocris Bioscience | 1128 |
| QX-314 | MilliporeSigma | 552233 |
| SR 95531 hydrobromide (Gabazine, GBZ) | Tocris Bioscience | 1262 |
| Tetrodotoxin (TTX) | Tocris Bioscience | 1069 |
| γ-Aminobutyric acid (GABA) | Tocris Bioscience | 0344 |
| Experimental models | | |
| *Fmr1* KO mice | Jackson Laboratory | 004624 |
| WT control mice | Jackson Laboratory | 004828 |
| Software and algorithms | | |
| Stim&Record | Custom software | N/A |
| LabView | National Instrument | LabView 8.6 |
| MATLAB | MathWorks | MATLAB 2012b |
| Origin | Origin Labs | Origin 8.5 |
| Mini Analysis | Synaptosoft Inc | Version 6.0.3 |